THE JOURNAL OF BONE & JOINT SURGERY (BRITISH)

Longitudinal limb deficiencies and the sclerotomes

AN ANALYSIS OF 378 DYSMELIC MALFORMATIONS INDUCED BY THALIDOMIDE

J. McCredie, H.-G. Willert

From the Royal Prince Alfred Hospital, Sydney, Australia and the Georg-August-Universität, Göttingen, Germany

The pathogenesis of longitudinal reduction deformities of the limbs, or dysmelia, is still a matter of debate. Their morphological pattern was defined from a large collection of radiographs of children with dysmelia following the thalidomide disaster.

We compared radiographs of 378 of these limbs with the sclerotomes which are areas of segmental sensory innervation of the limb skeleton defined by the radiation of referred pain. The pattern of dysmelia matched the sclerotomes closely in 279 limbs (73.5%).

The principles of skeletal reduction in dysmelia are explained by the arrangement of the sclerotomes. The congruence between two separate and independent data sets shows that both patterns are expressions of the underlying segmental sensory innervation of the skeleton, and that the sensory nervous system is involved in the process of limb morphogenesis and teratogenesis.

J Bone Joint Surg [Br] 1999;81-B:9-23.
Received 13 June 1997; Accepted after revision 14 October 1997

Most human limb deficiencies, whether sporadic or hereditary, have a wide range of dysmorphism. Because they are rare, individual cases of these malformations have been regarded as curiosities rather than as part of a biological spectrum. It was not until the thalidomide disaster that the underlying patterns were recognised. Even so, the wide variety of dysmorphism in early thalidomide children led to the belief that the distribution of these malformations was random.[1]

The large number of cases collected at that time has provided valuable material for analysis of the pattern underlying the malformations, and for determining how thalidomide worked. In a study of the nature, aetiology and pathology of what was named 'dysmelia',[1-4] Willert and Henkel[2,3] arranged a series of 287 thalidomide cases in order of increasing severity of limb reduction. Figures 1 and 2 summarise the pattern of the malformations[5] and the teratological sequences which emerged from that study. The defects were longitudinal, not transverse. They ranged from isolated peripheral hypoplasia to complete absence of the limb (amelia). The sequential longitudinal reduction of the limb skeleton obeyed certain principles:

1) Some bones as a whole, as well as defined areas within one bone, were more vulnerable than others.

2) In each limb the deficiencies occurred in a longitudinal axis of reduction.

3) There was a clear interdependence between proximal and distal parts of the limb.

In thalidomide-induced dysmelia, the deficiencies were characteristically on the radial side of the upper limb and the tibial side of the lower. In the upper limb, there was progressive reduction in, and loss of the bones of the thumb, radius and humerus which preceded the reduction of the ulna or the ulnar digits. In the lower limb, reduction began in the distal tibia or proximal femur, and affected the fibula and fibular digits last. Willert and Henkel stressed that there was a common entity, an underlying pattern which had many different but related manifestations. Since the old method of classification tended to mask this, a simpler system was proposed and is now widely accepted as an international standard.[5,6]

The morphological pattern of longitudinal skeletal reduction requires explanation. The peripheral skeleton may be divided longitudinally based on the segmental sensory nerve supply of the bones and joints. This pattern of innervation has been the subject of much research since the end of the last century, culminating in the publication of 'sclerotome maps' by Inman and Saunders in 1944[7] (Figs 3 and 4). These authors defined a sclerotome as a longitudinal band of skeletal structures supplied by one spinal segmental sensory nerve. Their maps were based on clinical and experimental studies of the radiation of deep referred pain from skeletal structures. The sclerotomes are the counterparts of dermatomes and myotomes and underlie but extend beyond the latter. Each sclerotome starts at the neuraxis and extends towards the periphery. Only the sixth, seventh and eighth cervical sclerotomes reach the hand; the fifth termi-

J. McCredie, MD, Visiting Radiologist
Department of Diagnostic Radiology, Royal Prince Alfred Hospital, New South Wales 2052, Camperdown, Australia.
H.-G. Willert, MD, Professor and Director
Georg-August-Universität, Orthopädische Klinik, Robert-Koch-Strasse 40, 37075 Güttingen, Germany.

Correspondence should be sent to Dr J. McCredie.

0301-620X/99/18448 $2.00

nates in the forearm near the elbow. In the leg, only the fifth lumbar and the first and second sacral sclerotomes reach the toes, while the fourth lumbar ends on the medial aspect of the tarsus and the third lumbar at the tibia below the medial side of the knee. Because of their longitudinal orientation, the sclerotomes cross joints and subdivide bones, including the pectoral and pelvic girdles, thus reorientating customary concepts of anatomy.

The sclerotomes are, like the dermatomes, normally invisible, but their presence should not be ignored. The vesicular eruption in herpes zoster, a viral infection of a segmental sensory nerve, renders the affected dermatome visible. Similarly, a sclerotome may be revealed by a disease of its nerve supply. McCredie has suggested the concept of 'sclerotome subtraction' for the radiological interpretation of reduction deformities of the limbs.[8,9] For instance, injury to the sixth cervical nerve in the embryo could inhibit development of the sixth cervical sclerotome, with defects in parts of the thumb, radius, humerus or scapula. Damage at the level of the fourth lumbar nerve in the embryo could reduce or subtract the fourth lumbar sclerotome, sparing the foot but reducing the tibia, femur and pelvis.

We have compared the sclerotome maps with the pattern of dysmelia in a large series of cases of thalidomide-induced limb defects. The skeletal deficiency in each limb was compared with the sclerotome map to determine whether or not the missing areas coincided with the sclerotomes. An attempt was made to judge if, or to what extent, these reduction defects could be interpreted by sclerotome subtraction.

We do not wish to discuss classification. The requirements for recording and labelling an individual case in a clinic differ from those needed to analyse a large series in search of a pattern of disease and a mechanism of pathogenesis.

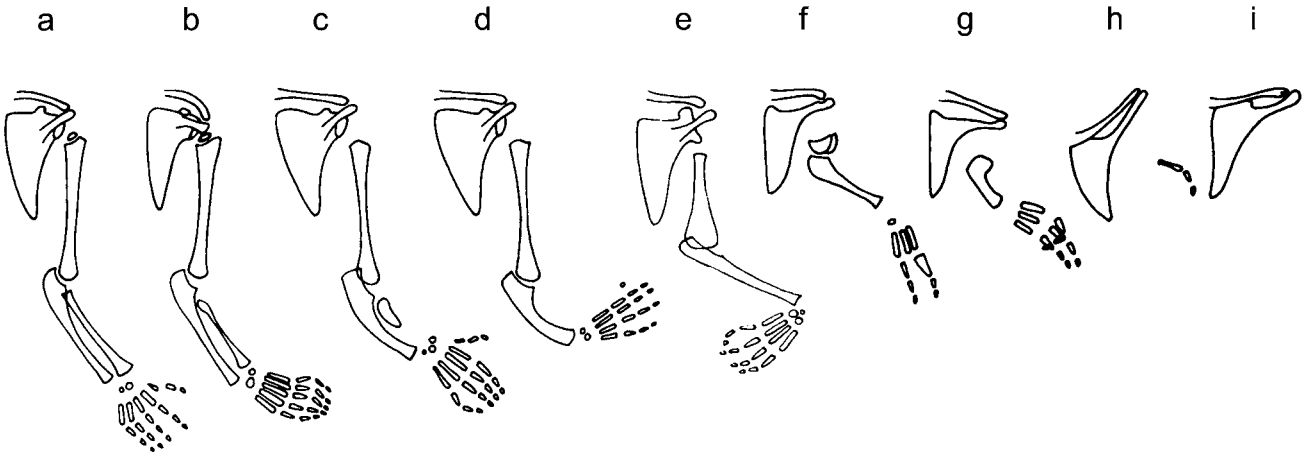

Fig. 1

The pattern of dysmelia in the upper limb showing the different stages.

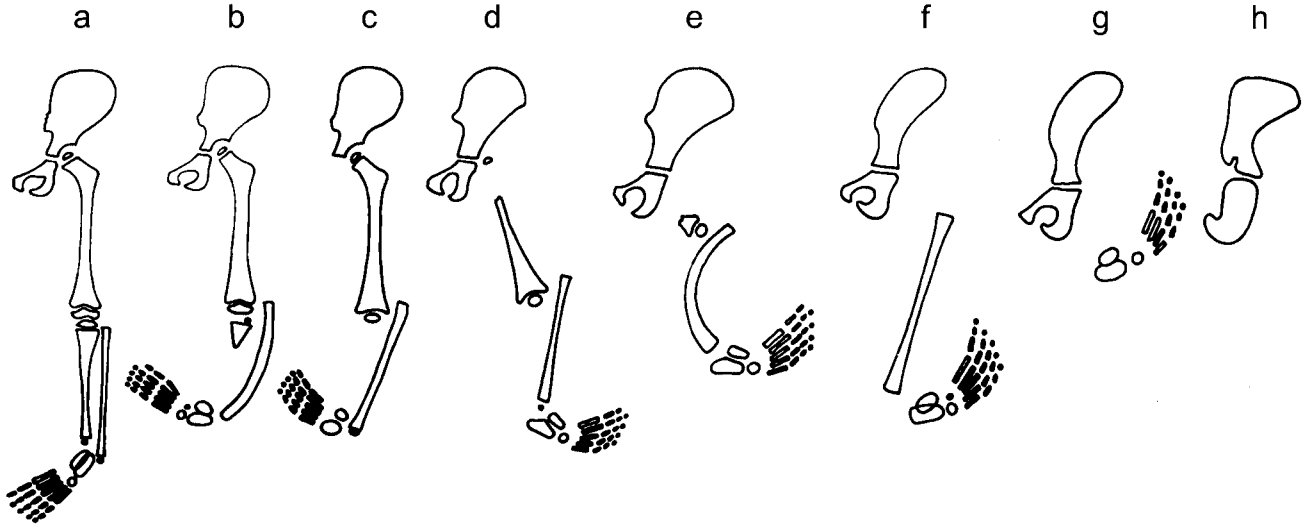

Fig. 2

The pattern of dysmelia in the lower limb showing the different stages.

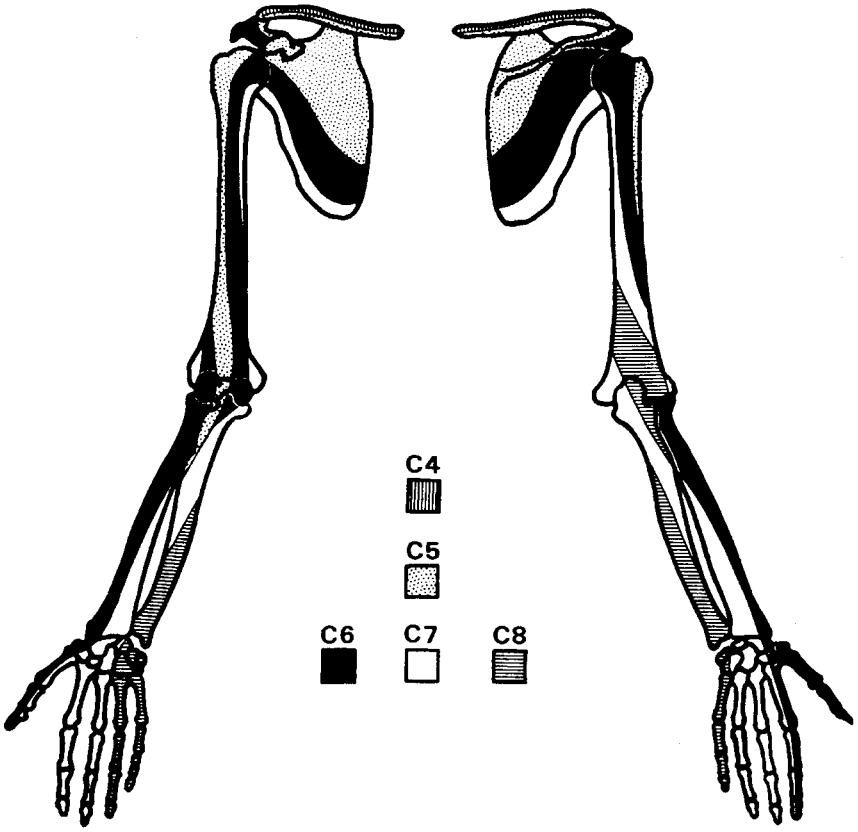

Fig. 3

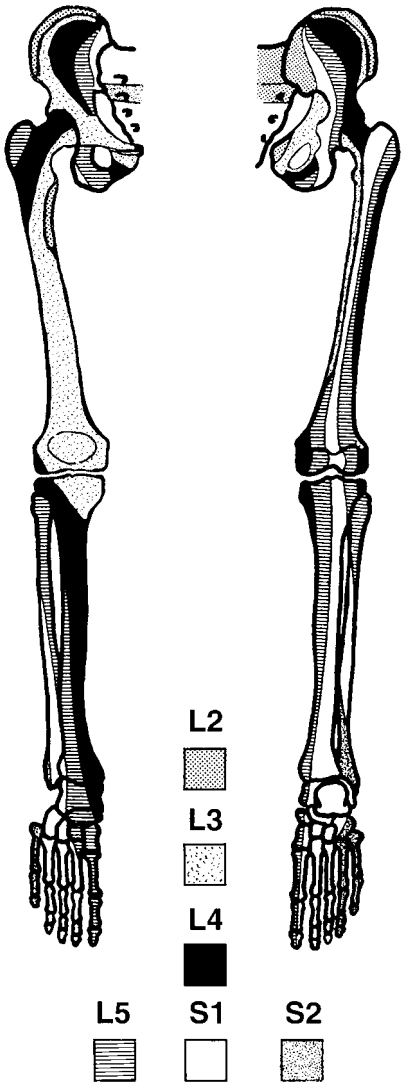

Fig. 4

Figure 3 – Anterior and posterior views of the sclerotomes of the upper limb (reproduced with permission from *J Nerv Ment Dis* 1944;99:660-7). Figure – 4 Anterior and posterior views of the sclerotomes of the lower limb (reproduced with permission from *J Nerv Ment Dis* 1944; 99:660-7).

Patients and Methods

We analysed the records of 378 limbs from 203 children with thalidomide embryopathy, collected by Willert and Henkel.[2-4] All the infants were born between 1958 and 1962 and had the typical signs of thalidomide embryopathy.[10-18] There were cases from several centres in Germany and some from Oxford, UK. Radiographs, or tracings of radiographs, had been filed with the essential clinical data including the name, date and place of birth, and the hospital attended.

In 180 infants we knew both the forenames and surnames, but in 23 only the initials were available and their sex was unknown. In nine the side of the malformation had not been recorded or marked on the radiograph or tracing.

In the 180 children in whom the sex was known, the male:female ratio was equal (91:89).

Isolated defects of the upper limbs predominated, being present in 85% of the children. Combinations of defects of the upper and lower limbs were seen in 12% and isolated defects of the lower limb in 3%. The ratio of involvement of upper:lower:both upper and lower limbs was 172:5:26.

Bilateral limb deficiencies were present in 90% with a high degree of symmetry within a limited range of morphology. Equal sex incidence, preponderance in the upper limb, and bilateral symmetry are features which have been noted in other series of thalidomide embryopathy.[10-18]

Henkel and Willert[3,4] used simple outline diagrams of the skeleton of the limb to record and analyse the anatomical features. Those bones or parts of bones which were missing from the radiograph were left out of the diagram. A working group of the International Society for Prosthetics and Orthotics agreed on a system of classification based on the principles outlined by Henkel and Willert,[5] and advocated that the deficiencies should be named after the skeletal elements which were absent. Swanson, Swanson and Tada[19] used a similar system, recording the condition on a

Table I. Results of sclerotome subtraction in 378 limbs with thalidomide-induced dysmelia. The 27 amelic limbs appear transverse (grade 3), but have been classified by experts as the final stage of longitudinal deficiency (grades 1 or 2). Therefore they are placed in each category in turn. Their classification makes no significant difference to the final result of the study. The pattern of dysmelia is closely matched by the sclerotomes in 73.5% to 80.8% of the limbs

	Number of limbs (%)		
Grade	**Amelia in grade 1**	**Amelia in grade 2**	**Amelia in grade 3**
1	306 *(80.8)*	279 *(73.5)*	279 *(73.5)*
2	56 *(15)*	83 *(22.3)*	56 *(15.0)*
3	16 *(4.2)*	16 *(4.2)*	43 *(11.5)*

silhouette drawing of the limb and skeletal parts with "shading out of absent parts" and naming the defect after them.

In our series of 203 cases there were satisfactory radiographic records of 378 limbs. A line diagram of the skeleton was assigned to each of these and the missing parts were shaded out. The deficiencies in skeletal structure were compared with the sclerotome maps to determine whether the morphology of the malformations and the sclerotomes coincided.

We attempted to grade the quality of fit between the sclerotomes and the malformations using three grades.

Grade 1. The longitudinal defect clearly coincided with the sclerotome map.

Grade 2. The longitudinal defect had a less obvious or ambivalent match with the sclerotomes.

Grade 3. The longitudinal defect coincided poorly or not at all.

Results

There was congruence of the missing bones with all or part of the sclerotomes (grade 1) in over 73% of cases (Table I). The match was less obvious in 15% (grade 2) and difficult in about 11% (grade 3). All had some evidence of sclerotome loss, even those with amelia.

A continuous pattern of deletion was seen in all malformations which was termed the "reduction tendency" by Henkel and Willert.[4] Within a large series, this continuous, gradual process of reduction is a slope rather than a series of steps, illustrating a smooth progression from a minimal distal reduction to total absence of the limb. Figures 1 and 2 show that the greater part of the skeleton is still present from stages a to f, with sufficient bony landmarks to identify readily the affected sclerotome or sclerotomes. It becomes more difficult to discern particular sclerotomes after stage f as the landmarks disappear.

Sclerotomes are easily identified distally, where the parallel digital rays and the paired bones of the forearm and lower leg provide obvious landmarks for establishing the identity of particular bones and bony remnants. Difficulties arise in the humerus and femur posteriorly, because here the sclerotomes tend to run in narrow parallel bands along these slender long bones.

Anatomical features allowing identification are absent in the diaphyses, which make it difficult or sometimes impossible to distinguish which part of the humerus or femur is missing.

Absence of all or part of a single sclerotome reduces the mass and shortens the shaft of an affected long bone, giving hypoplasia or partial aplasia. Subtraction of more than one sclerotome causes further loss of bone mass, progressive shortening of long bones and increasingly severe reduction of the limb. A reduction in mass of the major long bones brings the hand or foot closer to the trunk (phocomelia).

Gradually, the amount of skeleton remaining and the loss of normal landmarks are such that the identity of the residual sclerotomes becomes uncertain. Amelia is the most difficult subgroup to classify. At first sight, it appears to be a transverse rather than a longitudinal deficiency which would not fit into a system of classification of longitudinal defects. In the 27 amelic limbs in our series, however, the pectoral and pelvic girdles were always abnormal, with different degrees of hypoplasia, partial aplasia or dislocation (see Figs 12 and 16). Hypoplasia of the scapula was commonly associated with absence or hypoplasia of the glenoid process and clavicle. Absence of the acetabulum and incomplete formation of the pelvic bones were seen in hypoplasia of the pelvis. These girdle reductions indicated deficiencies in the proximal parts of the sclerotomes (Figs 3 and 4), yet they appeared to be disproportionately mild compared with the gross peripheral loss.

This apparent ambivalence of amelia has been discussed previously,[3,5,18,19] and all authors have concluded that amelia represents the ultimate stage of longitudinal limb deficiency. According to the Working Group of the International Society for Prosthetics and Orthotics[5] "the concept of progressive longitudinal reduction can be carried to a point where only a single digital remnant of a limb remains, and ultimately to the situation in which even this vestigial peripheral element failed to form – the true amelia. This, therefore, might be considered to be a maximum longitudinal deficiency, although presenting as a transverse type of defect". In order to accommodate the ambivalent appearance of amelia, we recorded our results as grades 1, 2 or 3 with three options (Table I). In spite of this ambiguity, the congruence of the sclerotomes with the pattern of dysmelia is still strong, between 73% and 80%. There were no cases which were not explained by the sclerotomes.

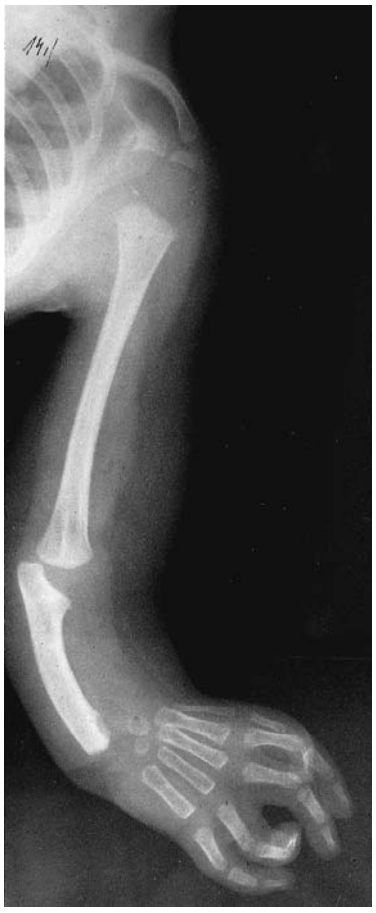

Fig. 5a

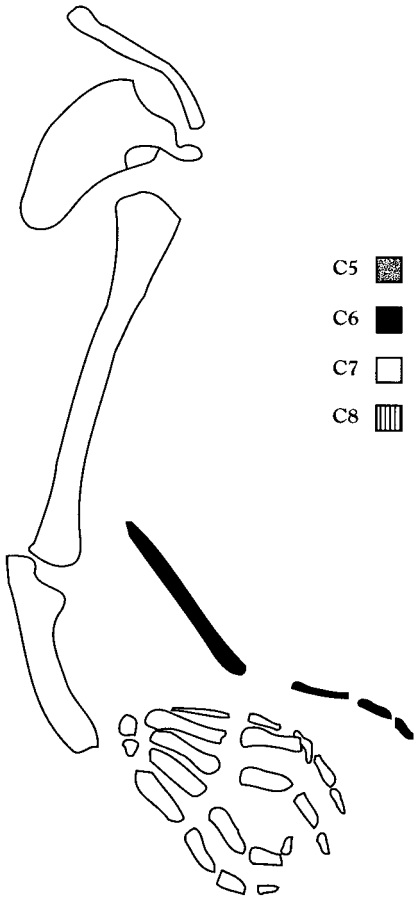

Fig. 5b

Figure 5a – Radiograph showing radial aplasia and a hypoplastic thumb. Figure 5b – Diagram showing subtraction of the sixth cervical sclerotome distally.

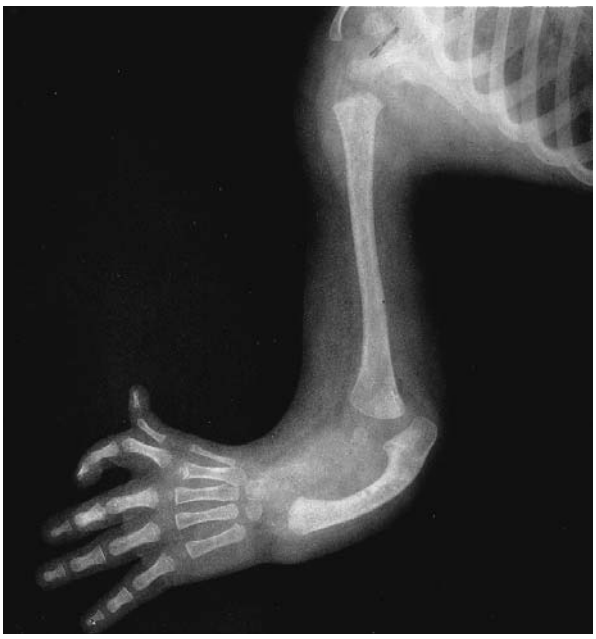

Fig. 6a

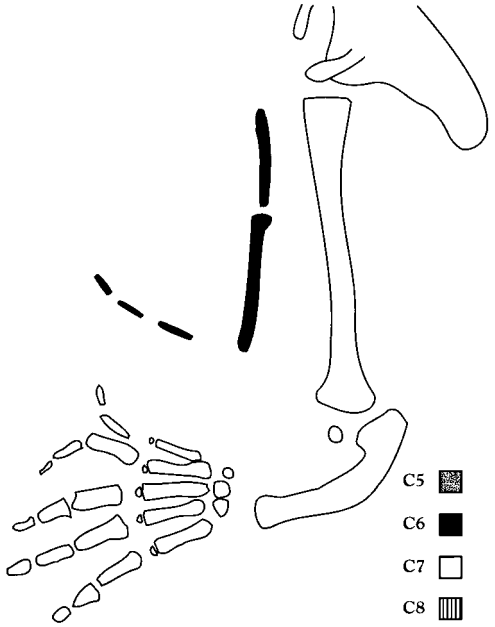

Fig. 6b

Figure 6a – Radiograph showing early involvement of the humerus, absence of the radius and a hypoplastic thumb with partial syndactyly. Figure 6b – Diagram showing subtraction of the proximal as well as the distal sixth cervical sclerotome.

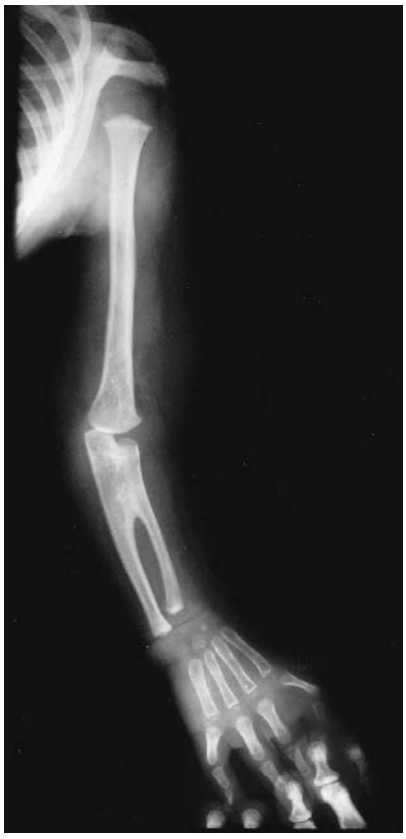

Fig. 7a

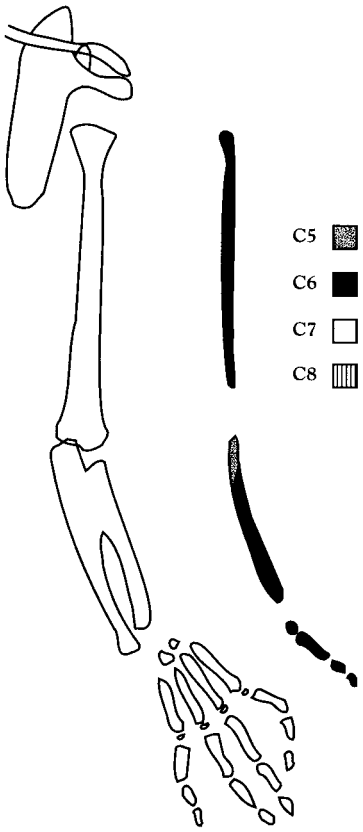

Fig. 7b

Figure 7a – Radiograph showing hypoplasia of the humerus and radius with proximal radio ulnar synostosis and an absent thumb. Figure 7b – Diagram showing subtraction of the fifth and sixth cervical sclerotomes.

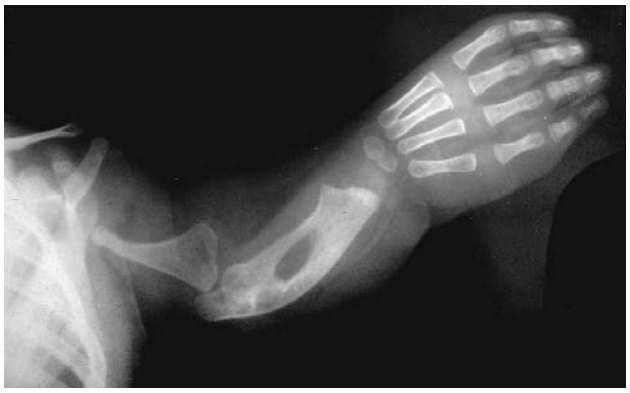

Fig. 8a

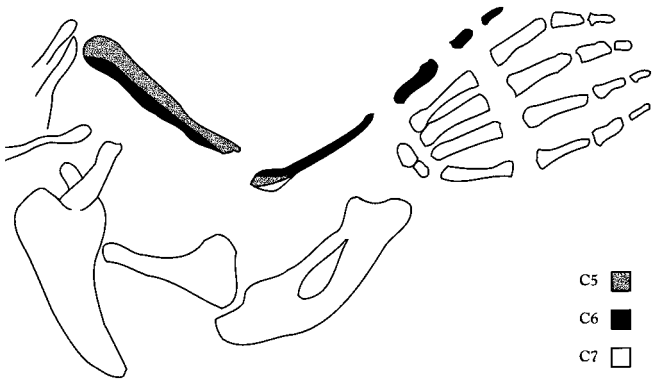

Fig. 8b

Figure 8a – Radiograph showing partial aplasia of the humerus involving the head and proximal shaft, hypoplasia of the radius, absence of the first ray of the hand and proximal and distal radio-ulnar synostosis. Figure 8b – Diagram showing total subtraction of fifth and sixth cervical sclerotomes.

UPPER LIMB

Sixth cervical sclerotome. Stages a to d of Figure 1 and Figure 3 illustrate deletion within the sixth cervical sclerotome, distally in the thumb or radius, proximally in the humerus, or involving all parts of the sclerotome. The thumb defects comprised absence, hypoplasia and triphalangism, and in some cases if the thumb was absent, hypoplasia of the index finger. The largest single group, 114 out of 330 (34.5%) malformations of the upper limb, involved only the sixth cervical sclerotome. Figures 5 and 6 illustrate two typical variants of reduction within this sclerotome. Grade-1 changes were seen in 102 limbs (89%) and grade-2 in 12 (11%); none had grade-3 changes.

Fifth and sixth cervical sclerotomes. The next stage in the reduction process is when the upper end of the humerus fails to form and the length of the bone is reduced. This was seen in 68 out of 330 (20.6%) malformations of the upper limb. The sclerotome maps show that this is deletion of the fifth and sixth cervical sclerotomes. The fifth terminates just distal to the elbow (Fig. 3) and does not reach the hand. Proximal radio-ulnar fusion indicates failure of separation of these two bones which lie within the distal part of

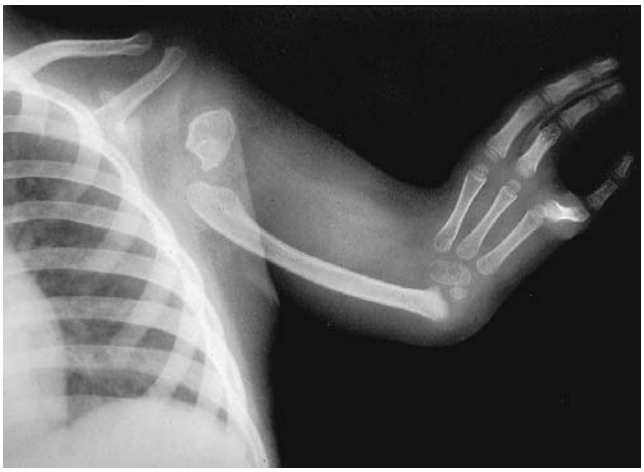

Fig. 9a

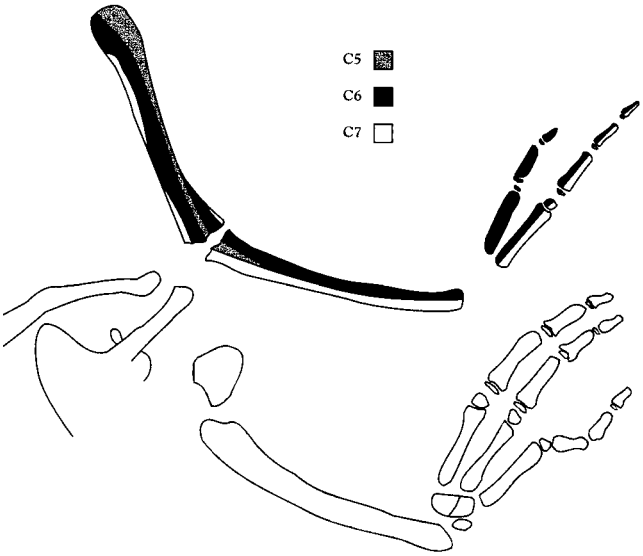

Fig. 9b

Figure 9a – Radiograph showing subtotal aplasia of the humerus and total aplasia of the radius and the first two rays of the hand. Figure 9b – Diagram showing subtraction of the fifth and sixth cervical sclerotomes and overlap on to part of the seventh. The elbow is present, indicating that the eighth remains together with the ulnar digits of the seventh and eighth.

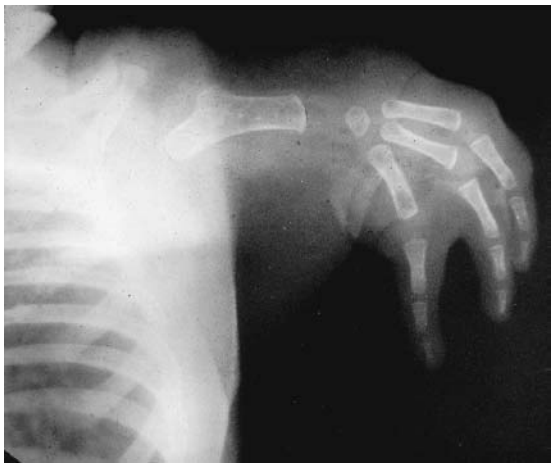

Fig. 10a

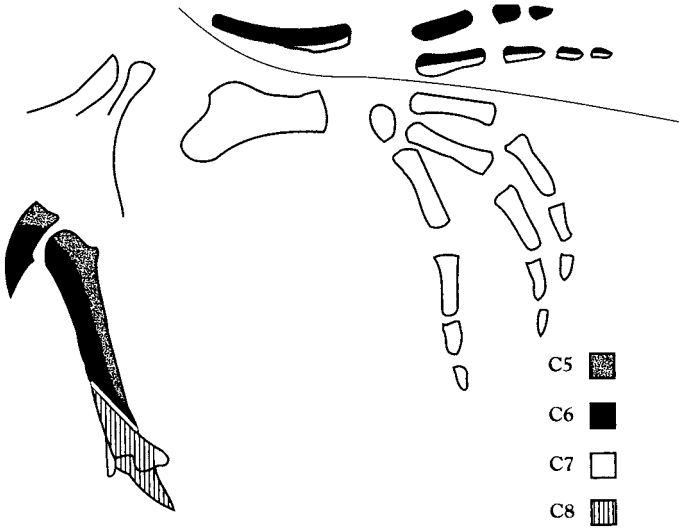

Fig. 10b

Figure 10a – Radiograph showing humeroulnar fusion, with three digits and few anatomical landmarks. Figure 10b – Diagram interpreted as subtraction of the fifth and sixth and part of the seventh and eighth cervical sclerotomes. The residual structures are those of the seventh and eighth.

the fifth cervical sclerotome. This minor degree of distal damage to the fifth is combined with reduction in the sixth cervical sclerotome as illustrated in Figures 7a and 7b. Further loss in the fifth cervical sclerotome subtracts mass and therefore length from the upper humerus without affecting the morphology of the hand. The shape of the fifth sclerotome is an inverted wedge with the base encompassing the head of the humerus and the apex tapering distally. Removal of this proximal wedge explains the shape of the residual distal humerus as shown in Figure 1, stage e and Figures 8a and 8b, a triangle based at the elbow with the apex proximal. Subtraction of the fifth as well as the sixth cervical sclerotome is potentially an effective way of reducing the length of the humerus and of accelerating the transition towards phocomelia. Grade-1 changes were present in 58 limbs (85%), grade-2 in seven (10%) and grade-3 in three (5%).

Fifth, sixth and seventh cervical sclerotomes. In 66 (20%) malformations of the upper limb the pattern was as shown in stage f of Figure 1. This illustrates deletion of the fifth, sixth and seventh cervical sclerotomes with some reduction of the eighth in the most severe examples. We saw no evidence of deletion of the seventh sclerotome in isolation, only in combination with the fifth and sixth, and

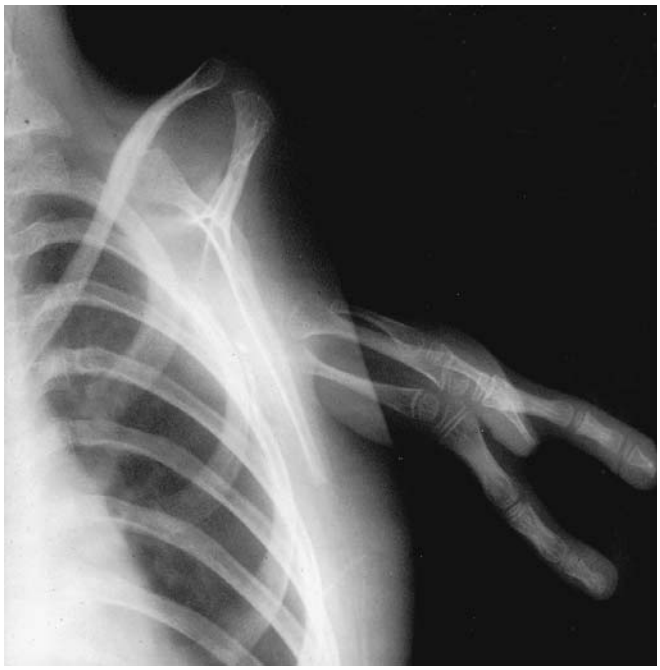

Fig. 11a

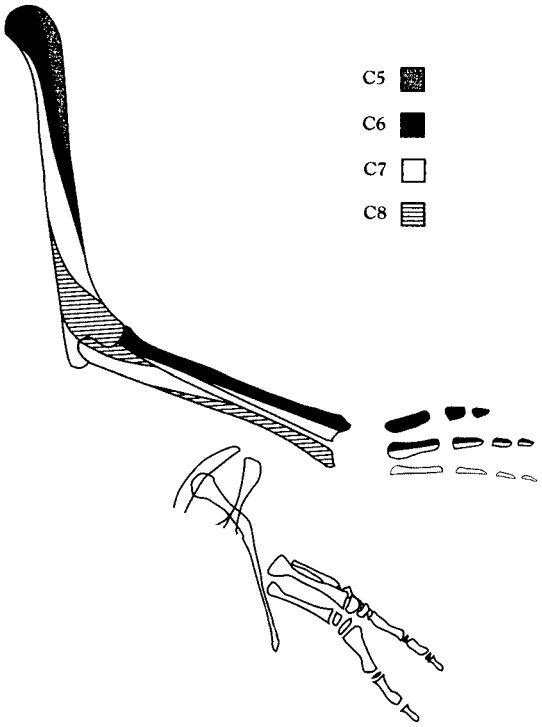

Fig. 11b

Figure 11a – Radiograph showing that all long bones and the first and second rays are absent. Figure 11b – Diagram showing that the remaining digits are probably the distal seventh and eighth sclerotomes. There is subtraction of the fifth, sixth and most of the seventh.

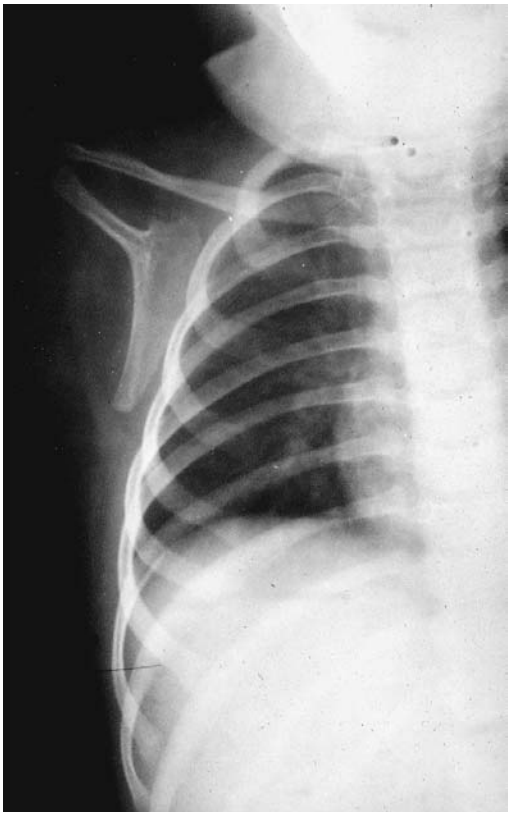

Fig. 12

Radiograph showing right upper amelia. There is hypoplasia of the scapula and absence of the glenoid process.

only when these were grossly involved. The remaining limb appears to be a combination of the eighth and part of the seventh sclerotome (Fig. 9). It could also, however, be interpreted as the seventh with part of the eighth since there is insufficient limb remaining to be certain which sclerotome forms the major part, but the elbow is derived from the eighth. Grade-1 changes were seen in 52 limbs (79%), grade-2 in 13 (19%) and grade-3 in one (2%).

Fifth, sixth and eighth cervical sclerotomes. There were 50 limbs (15%) in this category which is shown in Figure 1, stages g and h, and in Figure 10. The elbow is absent and the morphology of humeroradial fusion is thought to represent the residual seventh cervical sclerotome (Fig. 1, stage g). Further reduction leads to phocomelia (Fig. 11) including the single-digit form (Fig. 1, stage h). Here the residual row of phalanges clearly belongs to a distal sclerotome which has disappeared proximally, together with the fifth, sixth and seventh or eighth, respectively. This digit may belong to the seventh or eighth, but there is insufficient data for positive identification. Grade-1 changes were seen in 37 limbs (74%), grade-2 in ten (20%) and grade-3 in three (6%).

Fifth, sixth, seventh and eighth cervical sclerotomes. Amelia was seen in 24 (7%) of our upper limbs (Fig. 1, stage i and Fig. 12). It is the only apparently transverse deficiency in the typically longitudinal defects of thalidomide origin. Henkel and Willert,[2-4] Smithells and Newman[18] and Swanson et al[19] have all drawn attention to this apparent oddity pointing out that amelia should only be

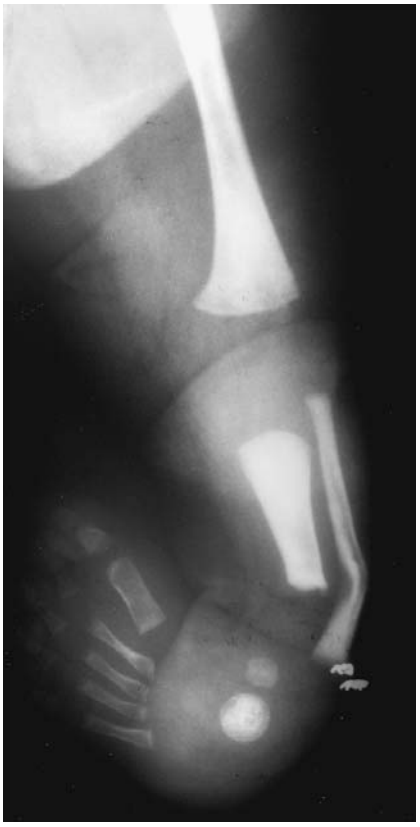

Fig. 13a

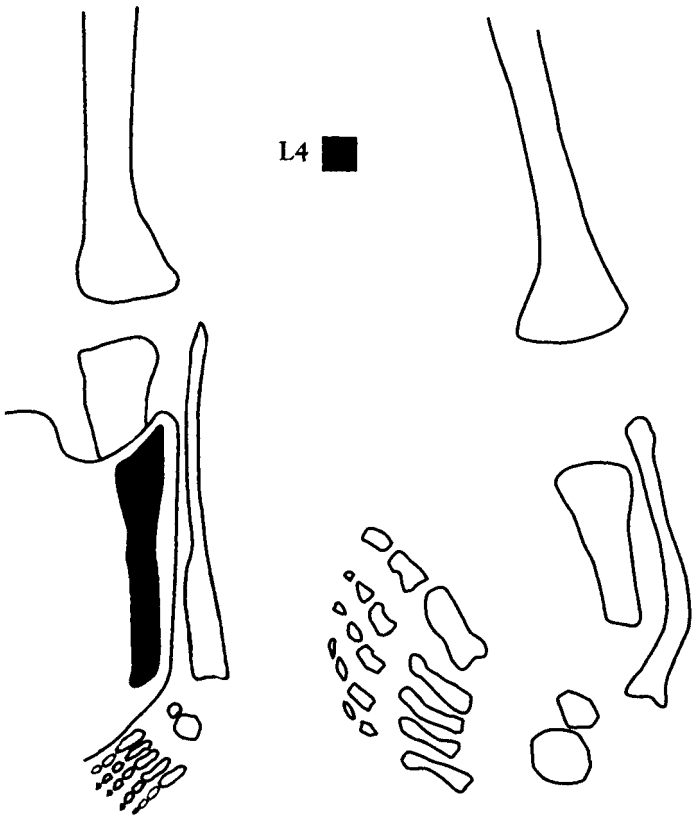

Fig. 13b

Figure 13a – Radiograph showing partial aplasia of the tibia with loss of the distal two-thirds. The foot is inverted. Figure 13b – Diagram showing subtraction of the fourth lumbar sclerotome.

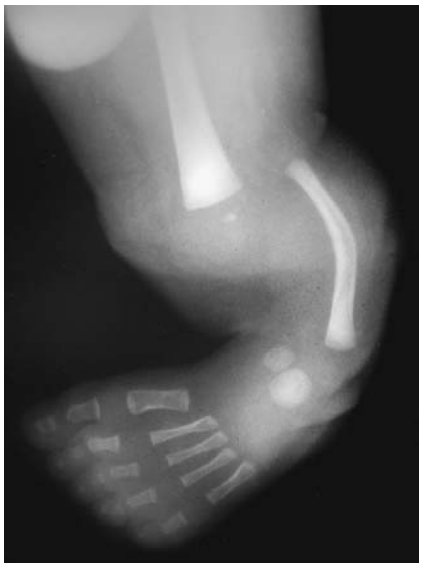

Fig. 14a

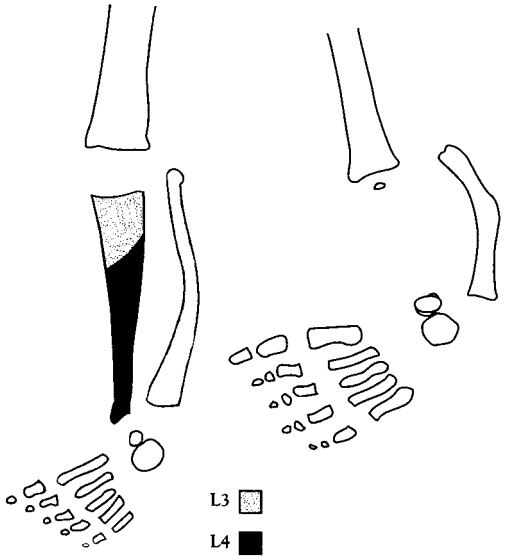

Fig. 14b

Figure 14a – Radiograph showing total aplasia of the tibia with an inverted foot. Figure 14b – Diagram showing subtraction of the distal third lumbar sclerotome as well as subtraction of the fourth.

classified as transverse if the pectoral or pelvic girdle is intact. If any parts of the limb girdles are deficient or hypoplastic it should be considered as a longitudinal deficiency of the most major degree. All our cases of amelia were associated with reduction in the limb girdle. In upper amelia the scapula was uniformly hypoplastic and the glenoid process absent or hypoplastic. These changes in the pectoral girdle had been emerging at earlier stages in the reduction as can be seen in Figure 1, stage e. The 24 limbs with upper amelia were interpreted as showing reduction in all sclerotomes although an order was less obvious than in malformations in which more skeletal material was left.

Other sclerotome combinations. The remaining eight upper limbs (2%) had malformations in which sclerotomes

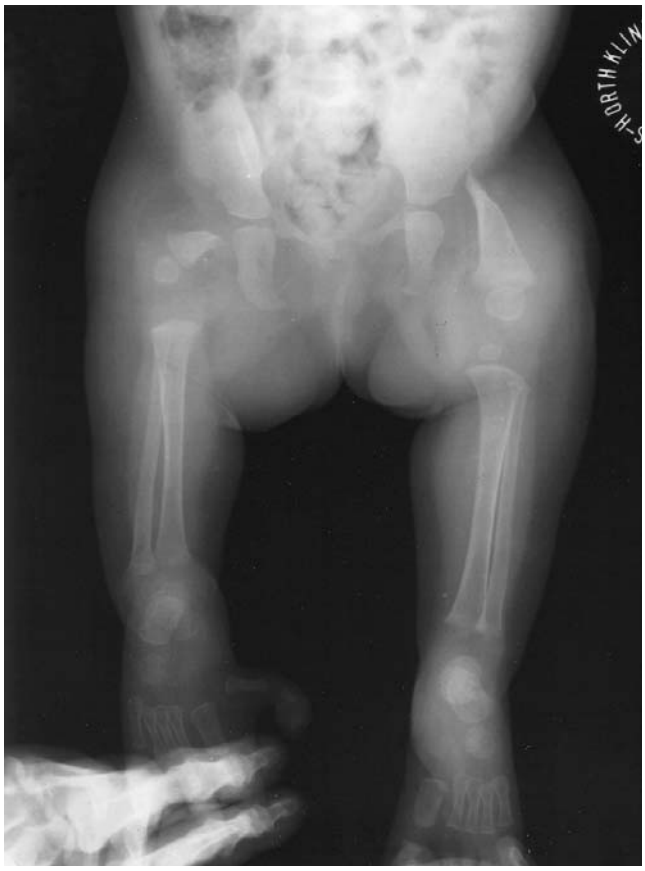

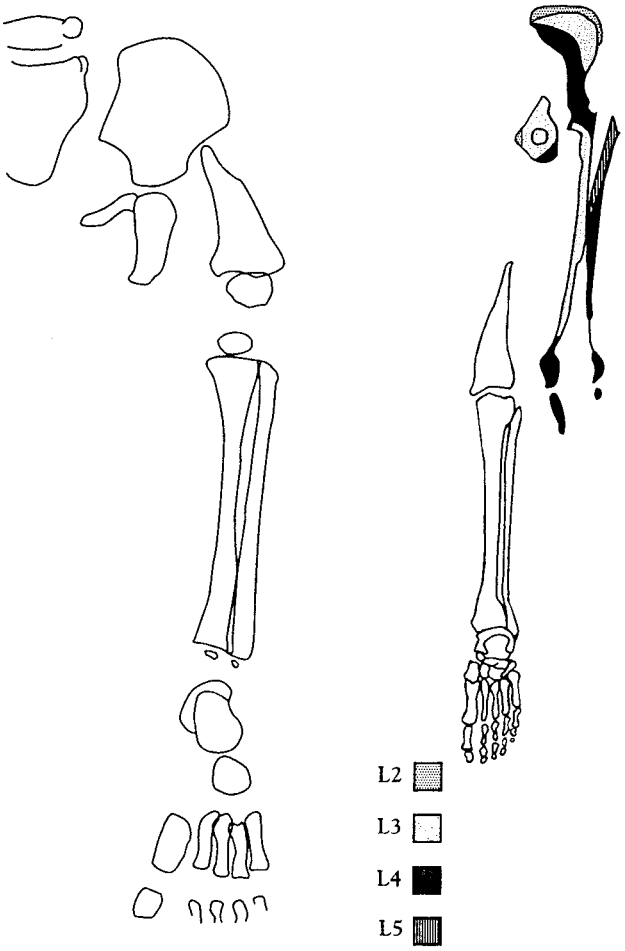

Fig. 15a

Fig. 15b

Figure 15a – Radiograph showing hypoplasia of the pelvis and partial aplasia of both femora. Figure 15b – Diagram interpreted as subtraction of the third and fourth lumbar sclerotomes proximally. The fifth lumbar and first and second sacral sclerotomes compose the distal femoral fragment and both the tibia and fibula reading from the posterior aspect of the map. Duplication of the left great toe illustrates irritation within the fifth lumbar sclerotome.

were difficult to identify. Four showed probable subtraction of the fifth cervical only; two retained the fifth with subtraction of the sixth, seventh, and eighth; one had subtraction of the fifth and eighth; and one limb the eighth only. Two had grade-1 changes, three grade-2 and three grade-3.

LOWER LIMB

There were 48 defects of the lower limb which followed the pattern of dysmelia as seen in Figure 2. This diagram can be compared with the sclerotome map of the lower limb (Fig. 4), working from left to right.

Fourth lumbar sclerotome. Figure 2, stages a and b, illustrates reduction in the distal part of the fourth lumbar sclerotome. The residual triangular fragment of the proximal tibia was a characteristic finding in all thalidomide series, and has been hitherto unexplained. The sclerotome maps reveal that it is the distal end of the third lumbar sclerotome which is made visible by disappearance of the fourth lumbar. Nine limbs (18%) had this appearance (Figs 13a and 13b), all classified as grade 1.

Third and fourth lumbar sclerotomes. Stages c, d and e of Figure 2 illustrate increasing degrees of reduction of the third and fourth lumbar sclerotomes. In the malformation shown in Figure 2, stage c, the distal part of the fourth lumbar sclerotome has disappeared together with the lower end of the third (Fig. 14). In stage d of Figure 2 the proximal part of the fourth lumbar sclerotome has also failed to form, leaving a quadrant of femoral head within a hypoplastic acetabulum. A long triangular remnant of the distal femur remains (Fig. 15). Both residual femoral fragments correspond to the proximal part of the third lumbar sclerotome anteriorly. The fifth lumbar and the first sacral sclerotomes are also incorporated into this triangular fragment posteriorly. When even more of the third lumbar sclerotome is subtracted the appearance is as shown in stage e of Figure 2 and Figure 15.

The acetabulum and the head and neck of the femur lie in the third and fourth lumbar sclerotomes. The distal triangular stump of the femur represents the fifth lumbar and first sacral components. The mass of the fibula is

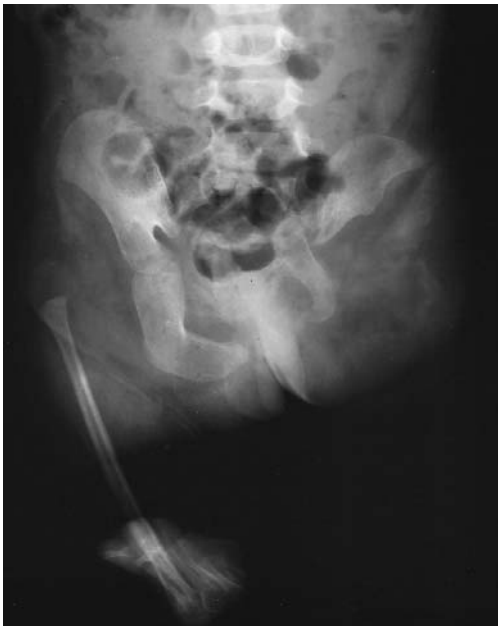

Fig. 16a

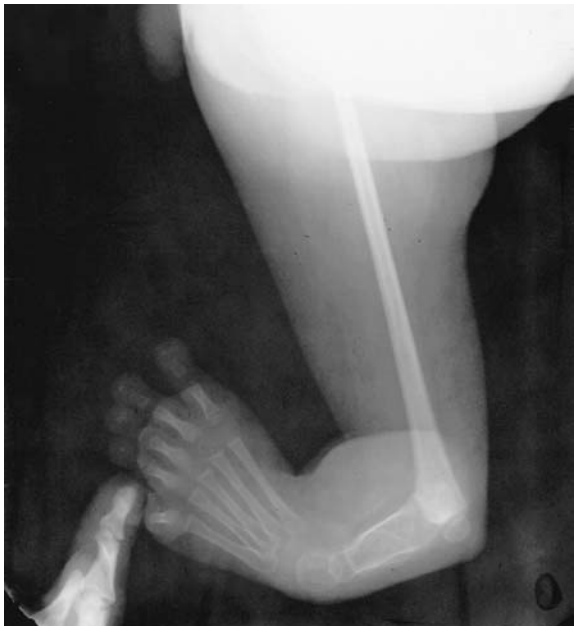

Fig. 16b

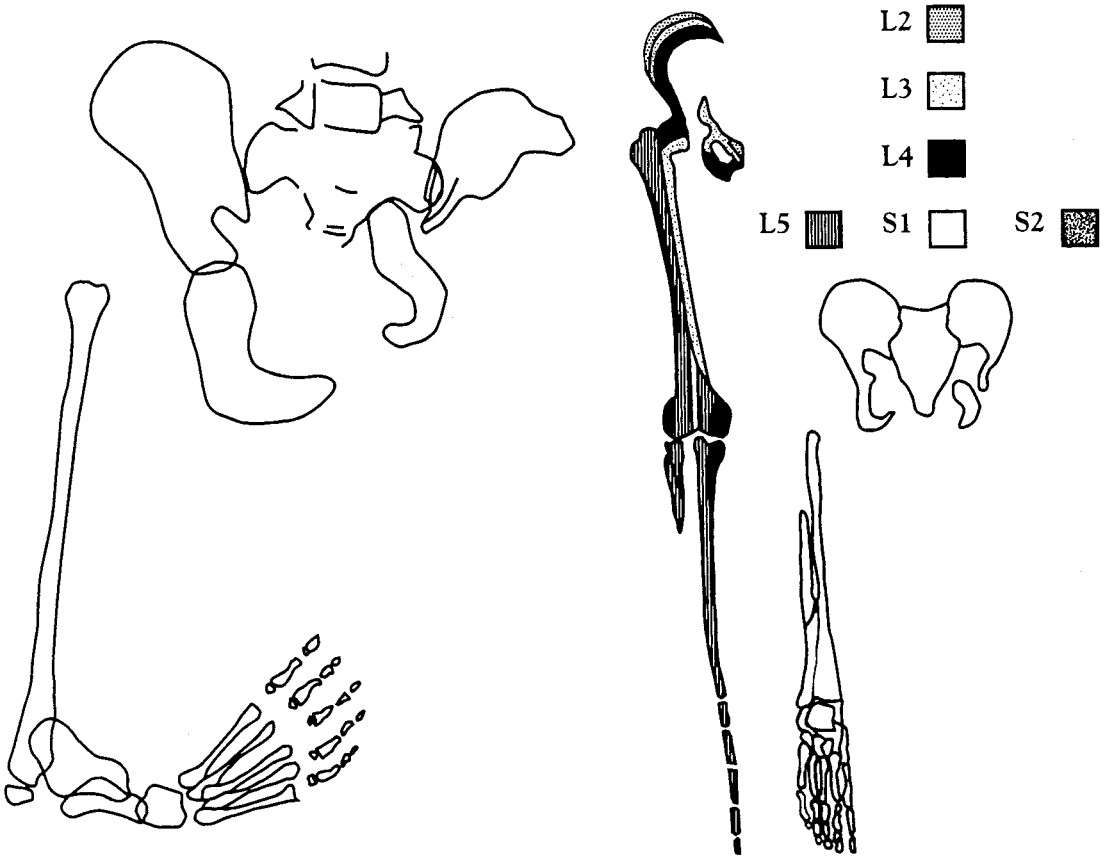

Fig. 16c

Figures 16a and 16b – Radiographs showing a) left lower amelia with defects and hypoplasia in the left pelvic girdle, no acetabulum on either side and no bone visible between the right fibula and the pelvis, and b) the complete bones of the inverted foot. Figure 16c – Diagram showing subtraction of the third, fourth and fifth lumbar sclerotomes. The remaining structures are distal parts of the first and second sacral sclerotomes. These seem to be the most resistant in the leg.

increased by incorporation of the fifth lumbar and first sacral sclerotomes from the posterior aspect of the tibia. The distal end of this composite bone carries a hypoplastic mortise joint for the ankle which was called the 'tibula' by orthopaedic surgeons at the time of the thalidomide disaster. In some cases, fusion of the tibial and fibular components did not occur, and the two bones remained separate, despite total reduction of the femur. This longitudinal proximal defect represents survival of the posterior sclerotomes, with loss of major parts of the anterior elements. The sclerotome map of the back of the leg shows that the fifth lumbar and first and second sacral can compose a tibia and fibula without the anterior third and fourth lumbar sclerotomes.

The commonest defect of the lower limb seen in 21 limbs (44%) in our series was deletion of the third and fourth lumbar sclerotomes to varying degrees as shown in stages c, d and e of Figure 2. Grade-1 changes were seen in 16 limbs (76%), grade-2 in two (10%) and grade-3 in three (14%).

Third, fourth and fifth lumbar sclerotomes. In 15 limbs (32%) the third, fourth and fifth lumbar sclerotomes were involved. These malformations are illustrated by stages f and g of Figure 2 with variations between them. There was no bone visible between the pelvis and the fibula (Fig. 16). The involvement of the fifth lumbar sclerotome sometimes included absence, hypoplasia, triphalangism or duplication of the hallux (Fig. 15). Deletion of other bones within the foot was not observed and the main structure was preserved until the last stage of reduction, when the sacral sclerotomes became involved in the reduction process. In one case there were three great toes.

Because the structure of the foot is little affected, difficulty in identification of individual digits does not occur in the lower limb. Limb reduction takes place within the major long bones and involves the deletion of the third and fourth lumbar sclerotomes which do not extend to the foot. Difficulties in interpretation can occur because of the inter-relationship of different sclerotomes on the anterior and posterior surfaces of the long bones. Six limbs (40%) had grade-1 changes, four grade-2 (26%) and five (33%) grade-3.

Third, fourth and fifth lumbar and first and second sacral sclerotomes. Three cases of amelia of the lower limb (6%) showed loss of all the sclerotomes in the leg (Fig. 2, stage h). In all cases there were hypoplastic malformations of the bony pelvis (Fig. 16).

The classification within each of the subgroups is shown in Figure 17.

Discussion

The patterns of dysmelia matched the sclerotomes exactly in approximately 75% of our cases. There was evidence of sclerotome subtraction in the remainder, but the congruence of the patterns was less exact (Table I). Our findings show that the absence of certain bones or areas within a bone can be explained by the sclerotomes. Some sclerotomes appeared to be more vulnerable than others, but within each subgroup of defects, there was a high correlation with the anatomy.

The longitudinal axis of reduction in each limb is very clearly explained by the sclerotomes. In the upper limb the sixth cervical sclerotome was involved in 98% (324/330) of cases, either alone or in combination with adjacent levels and is the axis of reduction in the arm. Thus, the sixth cervical is obviously most sensitive to thalidomide while the seventh cervical is the most resistant. All malformations of the lower limb showed subtraction of the fourth lumbar sclerotome. It was always the first to disappear, sometimes alone, but more often in combination with reduction in the adjacent third and fifth sclerotomes. It is the most sensitive to thalidomide and forms the axis of reduction in the leg. The sacral sclerotomes are the most resistant.

We do not know why the structures supplied by the sixth cervical and fourth lumbar nerves should be more sensitive to reduction by thalidomide than other segments. We have previously noted parallels in experimental teratology and phylogenesis[3,20] which suggest that younger phylogenetic acquisitions are more vulnerable. Thumb-finger opposition depends upon the sixth cervical nerve, and standing erect involves musculoskeletal structures supplied by the third

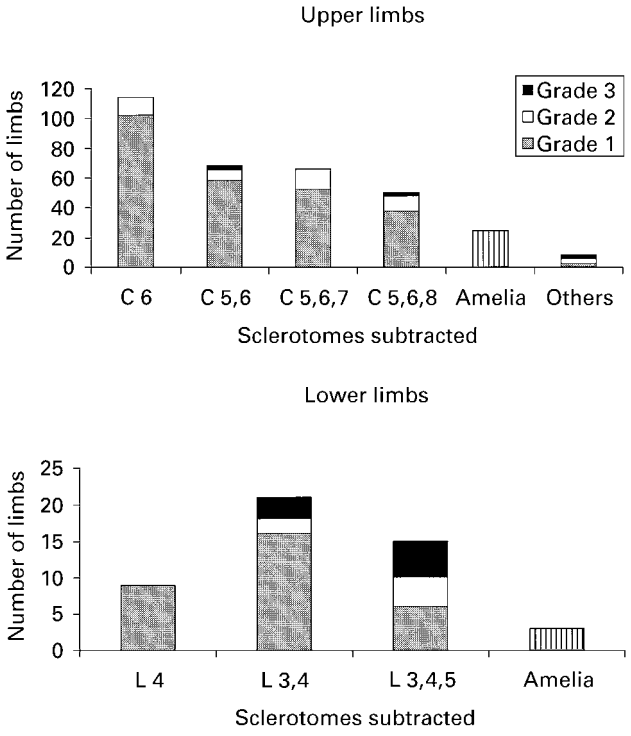

Fig. 17

Summary of the distribution and grades of fit of sclerotomes in 378 limbs with thalidomide-induced dysmelia. The scale of the diagram for upper limbs is reduced to accommodate the large number of cases. The 27 amelic limbs have not been committed to any one grade, but are incorporated into each in turn in Table I.

and fourth lumbar nerves. Both functions have been acquired relatively recently in evolution. Bretscher and Tschumi[21] have suggested that in the competition for expression between different structures in morphogenesis, success goes to those which have been established longest in evolution. Interdependence between the proximal and distal parts of the limb in dysmelia can be explained as progression within a sclerotome. It is possible to have proximal, distal or total lesions within one band of nerve supply, simulating the neurological distribution of segmental sensory neuropathies. Since the pattern of dysmelia coincides so well with the sclerotomes, both appear to be expressions of the underlying sensory segmental innervation of the skeleton. The action of thalidomide in the embryo reveals the existence of the sclerotomes which are otherwise invisible and indicates the involvement of the sensory nervous system in morphogenesis and teratogenesis.

The explanation as to how dysfunction of sensory nerves can disturb morphogenesis depends on the fact that sensory nerves have a trophic or growth-stimulating function which is separate from sensation.[22-27] In amphibia, sensory denervation prevents limb regeneration and thalidomide causes malformation in amphibian limb regenerates. While nerve impulses carrying sensation are electrical and centripetal, neurotrophism is believed to act centrifugally through axoplasmic flow.[26] It is not known whether neurotrophism is an additional property of nerves which transmit other sensory modalities, or whether there are dedicated trophic nerves within the sensory nervous system.

Thalidomide damages sensory nerves. It was recognised as a sensory neurotoxin in adults[28,29] before it was marketed as an antiemetic for early pregnancy. In adult patients with thalidomide neuropathy the symptoms of paraesthesia and anaesthesia were seen to persist for many years after medication had been stopped, the hallmark of a strong neurotoxin. The results of electrophysiological studies and sural nerve biopsies carried out during long-term follow-up showed that axonal degeneration occurs in thalidomide neuropathy.[30,31] Quantitative changes have been found in the peripheral nerves of the fetuses of thalidomide-exposed rabbits,[32,33] most marked in those with limb deformities. Neurotoxic injury to the neural crest or its derivatives could interfere with the trophic action on limb development, causing failure of growth in the structures supplied by the injured nerves.[20,34,35]

The preservation of the whole foot until the end of the reduction sequence warrants further comment. We are not convinced that the apical ectodermal ridge of the limb bud[36,37] plays a significant role in thalidomide embryopathy,[38] since if it did, the structures of the foot should be damaged from the early stages of the sequence. The resistance of the sacral sclerotomes to thalidomide explains the preservation of the foot. Interference with the function of the apical ectodermal ridge could not induce precise focal reduction of the radial digits and duplication of the great toe in radial and tibial dysmelias without damage to the other digits.

Many experiments have been carried out involving mechanical manipulation of limb buds, especially in the chick, but none has been able to model thalidomide embryopathy. The limb buds of the victims of thalidomide did not suffer surgical damage. Their maldevelopment was due to a toxic effect on a normal embryo, often inflicted at a stage before the appearance of the limb.

Malformation in the arm was seen after ingestion of thalidomide from the 24th day of gestation,[11] but in man the upper limb bud first arises from the trunk on the 28th day (Nishimura, 1972, personal communication), indicating that the pattern of morphogenesis of the limb is determined before the limb bud emerges from the trunk. This correlates with experimental findings which suggest that the positional specification of neural-crest cells occurs before they leave the neuroepithelium;[39] this has been established for the cranial neural crest, but not for the trunk or limbs. It is not known whether neuronal derivatives of the crest, such as sensory neurones, are similarly specified, nor is the role of HOX genes yet defined in the positional specification of neural-crest cells.[39] Trunk neural-crest cells, however, have been shown experimentally to be highly sensitive to environmental changes. This can restrict their ability to complete their differentiation into neurones, and influence the development of nerve-dependant derivatives such as skeletal structures.[40]

Genetic research has defined gene (homeobox) complexes related to particular segments of the central and peripheral nervous systems, common to several phyla, and including mammals.[41] The mechanism whereby homeobox genes pass morphogenetic messages to undifferentiated mesenchymal cells in the limb bud is not yet certain. One hypothesis proposes that undifferentiated cells in the embryonic limb buds communicate ‘positional information’ to one another. Even the proponents of this concept admit that “there is not a single case in all of vertebrate development where an intercellular signal has been unequivocally identified”.[42] The hypothesis of positional information has been coupled with that of a diffusable morphogen emitted from the zone of polarising activity (ZPA) of the ectodermal ridge of the limb bud. It is proposed that the genes in the mesoderm are switched on by a gradient of diminishing concentration of this morphogen as the cells are displaced proximally away from the ZPA by cell division. Evidence for the diffusable morphogen is “indirect”,[43] and evidence for ZPA as its source is “putative”.[44] “Little is known about the signalling mechanisms involved in such morphogenetic events”.[44]

The sensory nervous system is designed, in both structure and function, to transmit information in both directions between the central nervous system and the periphery. Proprioception is a sensory modality, not a property of mesoderm. In the human embryo the neural crest is present from the 18th day, ten days before the first appearance of

the upper limb bud, but during the sensitive period for thalidomide (days 21 to 42). Thus a mechanism which is known to be sensitive to thalidomide is present at an appropriate stage in morphogenesis for transmitting signals between the homeobox genes in the nervous system and the periphery. There is clear evidence that the neural crest plays an important role in limb morphogenesis.

The question arises as to why the possible role of sclerotomes in dysmelia was not considered at the time of the thalidomide disaster and its aftermath. There are at least two historical reasons for this.

First, sclerotome maps had been included in anatomy textbooks for only ten years (Inman, 1978, personal communication) and were not freely accessible at the time of the thalidomide tragedy. Secondly, after the work of Bardeen and Lewis in 1901,[45,46] there was a widespread belief that the limb bud of the embryo did not contain nerves and hence that the nervous system played no part in limb morphogenesis or teratogenesis. These authors reported that they did not observe axons in the limb buds of formalin-fixed embryos which had been embedded in paraffin and examined by light microscopy. These techniques are now known to destroy non-myelinated axons. They did not say that no nerves were present, although they are quoted as so doing.[47] This critical misquotation has been repeated in textbooks of embryology and in review articles,[48-50] and has diverted attention away from the peripheral nervous system in embryogenesis. The presence of nerves in the limb buds has subsequently been demonstrated using modern neurohistological techniques.[51,52] Unmyelinated axons have been shown by electron microscopy to ramify into the undifferentiated limb bud before any condensation of mesenchyme.

The sclerotome pattern is not confined to thalidomide-induced dysmelia. Other reduction deformities of the upper and lower limbs also follow the pattern of sclerotome subtraction.

The authors wish to thank the illustration departments of the Klinikum of the Georg-August Universität, Güttingen and the Royal Prince Alfred Hospital, Sydney and Satzspiegel, Bovenden, Germany for help with the preparation of the illustrations, and Frau Holländer of the Orthopaedic Department of the University of Güttingen for secretarial assistance. The Department of Radiology and the Administration of the Royal Prince Alfred Hospital, Sydney, provided study leave for research in Güttingen, Germany.

No benefits in any form have been received or will be received from a commercial party related directly or indirectly to the subject of this article.

References

1. **Wiedemann HR.** Current knowledge on embryopathies with exogenous malformations in man. *Medizinische Welt* 1962;1:1343-9.
2. **Willert H-G, Henkel L.** Die Dysmelie an den oberen Extremitäten. In: *Pathologie und Klinik in Einzeldarstellungen.* Berlin, etc: Springer-Verlag, , 1968.
3. **Willert H-G, Henkel L.** *Klinik und Pathologie der Dysmelie.* Exp Med Path und Klin Bd, vol 26. Berlin, etc: Springer-Verlag, 1969.
4. **Henkel L, Willert H-G.** Dysmelia: a classification and a pattern of malformation in a group of congenital defects of the limbs. *J Bone Joint Surg [Br]* 1969;51-B:399-414.
5. **Kay HW.** The proposed international terminology for the classification of congenital limb deficiencies. *Dev Med Child Neurol Suppl* 1975; 34:1-12.
6. **Henkel HL, Willert H-G, Gressmann C.** An international terminology for the classification of congenital limb deficiencies. *Arch Orthop Trauma Surg* 1978;93:1-19.
7. **Inman VT, Saunders JB de CM.** Referred pain from skeletal structures. *J Nerv Ment Dis* 1944;99:660-7.
8. **McCredie J.** Segmental embryonic peripheral neuropathy. *Pediatr Radiol* 1975;3:162-8.
9. **McCredie J.** Sclerotome subtraction: a radiological interpretation of reduction deformities of the limbs. *Birth Defects: original article series* 1977;XIII, 3 D:65-77.
10. **Lenz W.** Thalidomide and congenital abnormalities (Letter). *Lancet* 1962;1:45.
11. **Lenz W.** Das thalidomid syndrom. *Fortschr Med* 1963;81:148-55.
12. **Lenz W.** Epidemiology of congenital malformations. *Am NY Acad Sci* 1965;123:228-36.
13. **Pfeiffer RA, Kosenow W.** Thalidomide and congenital abnormalities. (Letter) *Lancet* 1962;1:45-6.
14. **Speirs AL.** Thalidomide and congenital abnormalities. *Lancet* 1962;1:303-5.
15. **Ministry of Health.** Reports on public health and medical subjects. No. 112. *Deformities caused by thalidomide.* London: HMSO, 1964.
16. **Cuthbert R, Speirs AL.** Thalidomide induced malformations: a radiological survey. *Clinical Radiol* 1963;14:163-9.
17. **Quibell EP.** The thalidomide embryopathy: an analysis from the U.K. *Practioner* 1981;225:721-6.
18. **Smithells RW, Newman CG.** Recognition of thalidomide defects. *J Med Genet* 1992;29:716-23.
19. **Swanson AB, Swanson GD, Tada K.** A classification for congenital limb malformation. *J Hand Surg Am* 1983;8:693-702.
20. **McCredie J.** Embryonic neuropathy: a hypothesis of neural crest injury as the pathogenesis of congenital malformations. *Med J Aust* 1974;1:159-63.
21. **Bretscher A, Tschumi P.** Gestufte Reduktion von chemisch behandelten Xenopus-Beinen. *Rev Suisse Zool* 1951;58:11.
22. **Singer M.** The nervous system and regeneration of the forelimb of adult triturus. II - the role of the sensory supply. *J Exp Zool* 1943;92: 297-312.
23. **Singer M.** The nervous system and regeneration of the forelimb of adult triturus. V - The influence of number of nerve fibers, including a quantitative study of limb innervation. *J Exp Zool* 1946;101: 299-337.
24. **Singer M.** The nervous system and regeneration of the fore limb of adult triturus. VI - a further study of the importance of nerve number, including quantitative measurements of limb innervation. *J Exp Zool* 1947;104:223-49.
25. **Singer M.** The influence of the nerve in regeneration of the amphibian extremity. *Quart Rev Biol* 1952;27:169-200.
26. **Singer M.** The trophic quality of the neuron: some theoretical considerations. In: Singer M, Schadé JP, eds. *Mechanisms of neural regeneration, progress in brain research.* Vol. 13, Amsterdam: Elsevier, 1964:228-32.
27. **Singer M.** Neurotrophic control of limb regeneration in the newt. *Ann NY Acad Sci* 1974;228:308-22.
28. **Fullerton PM, Kremer M.** Neuropathy after thalidomide ('distaval'). *Br Med J* 1961;2:855-8.
29. **Powell-Tuck GA.** Neuropathy after thalidomide ('distaval'). *Br Med J* 1961;2:1151.
30. **Fullerton PM, O'Sullivan DJ.** Thalidomide neuropathy: a clinical, electrophysiological and histological follow-up study. *J Neurol Neurosurg Psychiatry* 1968;31:543-51.
31. **Krücke W, von Hartrott H-H, Schröder JM, et al.** Light and electron microscope studies of late stages of thalidomide polyneuropathy. *Fortschr Neurol Psychiatr Grenzgeb* 1971;39:15-50.
32. **McCredie J, North K, de Iongh R.** Thalidomide deformities and their nerve supply. *J Anat* 1984;139:397-410.
33. **Dunlop GM, McCredie J.** Thalidomide, tibial nerves, and the threshold concept. In: Inoue S, et al, eds. Procs Sixth Marcus Singer Symposium, 1988.
34. **McCredie J.** Neural crest defects: a neuroanatomic basis for classification of multiple malformations related to phocomelia. *J Neurol Sci* 1976;28:3733-87.

35. McCredie J. Congenital fusion of bones: radiology, embryology and pathogenesis. *Clin Radiol* 1975;26:47-51.

36. Saunders JW. The proximo-distal sequence of origin of the chick wing and the role of the ectoderm. *J Exp Zool* 1948;108:363-403.

37. Tschumi PA. The growth of the hindlimb bud of Xenopus laevis and its dependence upon the epidermis. *J Anat (London)* 1957;91: 149-73.

38. Tabin CJ. A developmental model for thalidomide defects. *Nature* 1998;396:322-3.

39. Noden DM. Spatial integration among cells forming the cranial peripheral nervous system. *J Neurobiol* 1993;24:248-61.

40. Vogel KS, Marusich MF, Weston JA. Restriction of neurogenic ability during neural crest cell differentiation. *J Neurobiol* 1993;24: 162-71.

41. Gehring WJ. Homeo boxes in the study of development. *Science* 1987;236:1245-52.

42. Wolpert L. Do we understand development? *Science* 1994;266: 571-2.

43. Tickle C, Alberts B, Wolpert L, Lee J. Local application of retinoic acid to the limb bud mimics the action of the polarising region. *Nature* 1982;296:564-6.

44. Dollé P, Izpisua-Belmonte JC, Falkenstein H, Renucci A, Duboule D. Coordinate expression of the murine HOX-5 complex homeobox-containing genes during limb pattern formation. *Nature* 1989;342: 767-72.

45. Bardeen CR, Lewis WH. The development of the limbs, body wall and back in man. *Am J Anat* 1901;1:1-36.

46. Lewis WH. The development of the arm in man. *Am J Anat* 1902;1: 145-83.

47. Gardner E, O'Rahilly R. Neural crest, limb development and thalidomide embryopathy. *Lancet* 1976;1:635-7.

48. O'Rahilly R, Gardner E. The timing and sequence of events in the development of the limbs in the human embryo. *Anat Embryol Berl* 1975;148:1-23.

49. Poswillo D. Mechanisms and pathogenesis of malformation. *Br Med Bull* 1976;32:59-64.

50. Wolpert L. Mechanisms of limb development and malformation. *Br Med Bull* 1976;32:65-70.

51. Cameron J, McCredie J. Innervation of the undifferentiated limb bud in rabbit embryo. *J Anat* 1987;134:795-808.

52. McCredie J, Cameron J, Shoobridge R. Congenital malformations and the neural crest. *Lancet* 1978;2:761-3.